Draft version October 25, 2005
Preprint typeset using LaTeX style emulateapj v. 04/21/05

STAR FORMATION RATES IN COOLING FLOW CLUSTERS: A UV PILOT STUDY WITH ARCHIVAL XMM-NEWTON OPTICAL MONITOR DATA

A.K. Hicks[1] and R. Mushotzky[2]

Draft version October 25, 2005

ABSTRACT

We have analyzed XMM-Newton Optical Monitor (OM) UV (180-400 nm) data for a sample of 33 galaxies. 30 are cluster member galaxies, and nine are central cluster galaxies (CCGs) in cooling flow clusters having mass deposition rates between $8 - 525\ \mathrm{M}_\odot\ \mathrm{yr}^{-1}$. By comparing the ratio of UV to 2MASS J band fluxes, we find a significant UV excess in many, but not all, cooling flow CCGs, consistent with several previous studies based on optical imaging data (McNamara & O'Connell 1989; Cardiel, Gorgas, & Aragon-Salamanca 1998; Crawford et al. 1999). This UV excess is a direct indication of the presence of young massive stars, and therefore recent star formation. Using Starburst99 model of continuous star formation over a 900 Myr period, we derive star formation rates of $0.2 - 219\ \mathrm{M}_\odot\ \mathrm{yr}^{-1}$ for the cooling flow sample. For 2/3 of this sample it is possible to equate Chandra/XMM cooling flow mass deposition rates with UV inferred star formation rates, for a combination of starburst lifetime and IMF slope. This is a pilot study of the well populated XMM UV cluster archive and a more extensive follow up study is currently underway.

Subject headings: cooling flows—galaxies:clusters:general—galaxies:elliptical and lenticular, cD—galaxies:stellar content—stars:formation—ultraviolet:stars

1. INTRODUCTION

The 'mystery' of cooling flows (Fabian et al. 1984; Sarazin 1986; Fabian 1994) has baffled astronomers for over 20 years. Though the X-ray temperature often drops by a factor of three within the central 100 kpc (Allen et al. 2001), there is seldom enough mass at temperatures cooler than ~ 2 keV to be consistent with constant pressure cooling flow models. Recent XMM and Chandra results show that the distribution of temperature vs. emission measure also does not match the prediction of these models (Peterson et al. 2003; Voigt & Fabian 2004). While these results have reduced the implied cooling rate in most clusters, there is still a discrepancy of an order or magnitude or more between the X-ray cooling rates and the observed star formation rates (SFR) in many clusters. Contrary to conventional wisdom that there is no star formation at all in the central cluster galaxies, a number of studies have found significant star formation (Melnick, Gopal-Krishna, & Terlevich 1997; Smith et al. 1997; Hansen, Jorgensen, & Norgaard-Nielsen 1998; Mittaz et al. 2001; McNamara et al. 2004a; O'Dea et al. 2004; McNamara 2004b). However we are still far from a complete reconciliation between X-ray mass deposition rates and alternatively derived star formation rates in the majority of cooling flow clusters.

While many cluster cooling flows have been well observed in the radio and with emission line studies (Heckman et al. 1989, and others) there have been very few published studies of the UV properties of cooling flow clusters. We use archival XMM Optical Monitor UV observations to derive the UV luminosities of a moderate sample of clusters. Since the dominant contribution to UV flux comes from short-lived main sequence stars, and the total number of these stars is directly proportional to the star formation rate (Kennicutt 1998) the UV is one of the prime routes to understanding star formation. We address and quantify the connection between cooling flows and star formation in our pilot sample. Unless otherwise noted, this paper assumes a cosmology of $H_0 = 70$ km s^{-1} Mpc^{-1}, $\Omega_M = 0.3$, and $\Omega_\Lambda = 0.7$

[1] Center for Astrophysics and Space Astronomy, University of Colorado, Campus Box 389, Boulder, CO 80309; ahicks@alum.mit.edu
[2] Goddard Space Flight Center, Code 662, Greenbelt, MD, 20771; richard@milkyway.gsfc.nasa.gov

2. THE XMM-NEWTON OPTICAL MONITOR

The XMM Optical/UV Monitor is a modified 30cm Ritchey-Chretien telescope mounted alongside the X-ray mirror modules (Mason et al. 2001) allowing simultaneous X-ray and UV/optical observations over the central 17 square arcminute region of the X-ray field of view. The 256×256 pixels have an angular resolution of $\sim 1''$. The sensitivity limit of the Optical Monitor (OM) is 24 mag. This study utilizes the UVW1 filter (220-400 nm), along with the UVW2 (180-260 nm) and UVM2 (200-280 nm) filters for calibration purposes. Previous XMM OM studies of clusters have been limited to the detection of UV emission in Abell 1795 (Mittaz et al. 2001).

3. SAMPLE AND OBSERVATIONS

Our pilot sample consists of 33 galaxies and eleven clusters. Three of them (M49, M60, and M86) were selected because they possess IUE photometric information (Burstein et al. 1988) and were used to compare OM to IUE fluxes. 21 galaxies in the IC 1860 and Coma fields were used to calibrate the relationship between UV and IR luminosities in passively evolving early type and cD galaxies. Two UVW1 observations of Coma were included, one centered on the cDs, and one which is off-center but contains numerous early-type galaxies.

The remaining nine clusters in our sample were chosen because of significant X-ray determined mass deposition rates, general overlap with the samples of McNamara & O'Connell (1989) and Cardiel, Gorgas, &

Aragon-Salamanca (1998), moderate to low redshift, inclusion in the 2MASS galaxy sample, with archival XMM UVW1 data. The majority are low redshift objects ($z < 0.1$), but we also include three moderate redshift clusters ($z \sim 0.25$) which have very strong cooling flows. Figure 1 shows one of the cooling flow clusters in our sample, with XMM-Newton UVW1 contours overlaid. Table 1 lists the objects in our current sample, their redshifts, relevant filters, and OM exposure times.

4. SURFACE BRIGHTNESS

We fitted the flux in concentric circles around the emission peak of each galaxy to a radial surface brightness profile of the form: $I(r) = I_0\ (1 + r^2/r_0^2)^{1/2-3\beta} + I_B$ Where I_0 is the normalization, r_0 is the core radius, and I_B is a constant representing the background contribution. The surface brightness profiles are well fit by these models (Figure 2). Fit parameters are given in Table 2.

5. PHOTOMETRY

We retrieved pipeline-processed UV data from the XMM-Newton Science Archive and combined observations with the same pointing. For our calibration sample we used a circular aperture of $7''$ radius, a reasonable approximation of the IUE aperture (Burstein et al. 1988), and the size of the fixed 2MASS photometric aperture. The data were corrected for background using a $35''$ radius background region taken from an outlying area of the chip in the same observation. The fluxes were determined from the OM counts-to-flux conversions, and errors are $\sqrt{\mathrm{N}}$ photon statistics.

The results from UVW2 and UVM2 observations of M49, M60, and M86 were compared with the IUE determined flux value of each object (Burstein et al. 1988) for the bandpass of the appropriate filter. Our results are consistent with theirs to within $< 35\%$, errors similar to those of Vassiliadis et al (1996) and Koratkar et al. (1997). Two of the three galaxies have lower OM fluxes than IUE fluxes, indicating that the Optical Monitor does not have a red leak.

We determined UVW1 fluxes for the rest of our sample (see Table 1), for a $7''$ radius region, as described above. The UVW1 data were corrected for galactic extinction (Cardelli, Clayton, & Mathis 1989) and J band extinction values were retrieved from the NASA/IPAC Extragalactic Database (NED).

6. CALIBRATION

The low redshift ($z \sim 0.023$) calibration sample has 23 galaxies in IC 1860 and Coma with 2MASS J band photometric measurements. Two of these galaxies exhibited high UV fluxes with respect to the rest of the calibration sample, and were described as star forming in a FOCA study Donas, Millard, & Laget (1995) thus are not appropriate for inclusion in our UV/IR luminosity calibration of passively evolving early type galaxies, and were removed from the remainder of this study.

A least squares fit between the UVW1 and J band luminosities for the remaining 21 early type galaxies is well described by a simple powerlaw: $\mathrm{L_{UV}} = C_1 \times \mathrm{L_{IR}}^{C_2}$, where $\mathrm{L_{UV}}$ is the UVW1 luminosity and $\mathrm{L_{IR}}$ is the 2MASS J band luminosity, inside $7''$ radius apertures with $C_1 = 0.090 \pm 0.007$ and $C_2 = 0.708 \pm 0.007$ (Figure 3). We use this correlation to predict the UV light from non-starforming, passive galaxies assuming that the UV light from such objects is produced by old evolved stars coming from the same population that produces the IR light.

7. PHOTOMETRIC RESULTS

The UV luminosity excesses of the cD galaxies in the nine cooling flow clusters were calculated by subtracting the expected UV light due to old stars (from Section ??) from the measured UV luminosity of each cluster. Figure 4 shows the J band luminosity of each galaxy in our sample vs. its UV/IR luminosity ratio. We do not estimate or correct for internal dust absorption, and thus these values place a lower limit on excess UV emission.

The data from a single filter do not allow one to break the degeneracy between age and mass of the young stellar populations. We folded through the UVW1 filter Starburst99 (Leitherer 1999) redshifted models corresponding to continuous star formation over a a variety of timescales with solar abundance (Z = 0.020) and IMF powerlaw indices of both 2.35 and 3.3, to establish the relation between OM UV counting rates and star formation rate. The measured UV luminosity excesses of the clusters were then used to estimate per-year star formation rates (Table 3) and were compared to X-ray derived mass deposition rates from Voigt & Fabian (2004), Peterson et al. (2003), and R. Mushotzky (2005, private communication). Also in Table 3 are estimates of the duration of continuous star formation, and best fitting IMF powerlaw index. These values were derived by plotting the relationship between star formation duration and rate for each given UV excess and IMF slope, then finding the set of parameters (slope and duration) at which X-ray determined mass deposition rates intercepted those curves. The 900 Myr models should be closest to the average lifetime of a cooling flow (Allen et al. 2001).

8. SUMMARY AND DISCUSSION

There is a significant UV luminosity excess in the central galaxies of most cooling flow clusters, implying that star formation has recently been or is currently occurring, most likely as a direct result of radiative cooling of the intracluster medium (ICM). These conclusions are qualitatively consistent with previous optical imaging studies of star formation in cooling flow clusters (McNamara & O'Connell 1989; Cardiel, Gorgas, & Aragon-Salamanca 1998; Crawford et al. 1999).

In the absence of multiwavelength spectral information, it is difficult to constrain a particular model of the star formation history of these galaxies. However we note that for 2/3 of our sample it is possible to find some combination of the parameters of IMF slope and starburst lifetime which allow equal X-ray determined mass deposition rates and UV inferred star formation rates.

In none of the OM, Chandra or HST images is there evidence of a significant excess central flux, implying the AGN UV contribution to our signal is small. In addition, the amount of UV flux which might come from the cooling flow itself, is much smaller than measured UV excesses. Since the calibration sample consists entirely of low redshift early type galaxies, there is a possible systematic error in our calculations of the SFRs of the three moderate redshift ($z \sim 0.25$) clusters in our sample, due to evolution in the UV luminosity of the old stellar population (Brown et al. 2003) and/or uncertainties in the redshift evolution of the star forming component.

While there is significant UV flux in 2/3 of our cooling flow sample, 1/3 of the objects with significant cooling rates from modern data do not have detectable UV excesses, and the ratio of UV light to X-ray cooling rate (Figure 5) shows a wide range. The origins of this scatter are unclear and a larger UV sample, with direct comparison of X-ray and radio imaging and IR data, is necessary to get a clearer picture. The discovery of copious UV emission from several cooling flow clusters confirms the previous work and shows that a significant fraction of the cooling gas in clusters can indeed form stars.

Our star formation estimates are very basic, based solely on a simple conversion from UV light to SFR (Kennicutt 1998). We have bypassed issues of the age of the star formation, the effects of reddening, the slope of the IMF and metallicity effects. More and better data (such as could be obtained by Galex or HST spectroscopy) is necessary to determine precise star formation rates.

This paper is a pilot study and we are now analyzing more of the OM UV filters and including the many additional clusters in the archive. This large sample will allow a more thorough characterization of recent star formation in cooling flow clusters of galaxies.

REFERENCES

Allen, S.W., Schmidt, R.W., & Fabian, A.C., 2001, MNRAS, 328, 37
Birzan, L., Rafferty, D.A., McNamara, B.R., Wise, M.W., & Nulsen, P.E.J. 2004, ApJ, 607, 800
Brown, T.M. et al. 2003, ApJ, 584, 69
Burstein, D., Bertola, F., Buson, L.M., Faber, S.M., & Lauer, T.R. 1988, ApJ, 328, 440
Byrd, G., & Valtonen, M., 1990, ApJ, 350, 89
Cardelli, J.A., Clayton, G.C., & Mathis, J.S. 1989, ApJ, 345, 245
Cardiel, N., Gorgas, J., & Aragon-Salamanca 1998, MNRAS, 298, 977
Crawford, C.S. et al. 1999, MNRAS, 306, 857
Donas, J., Millard, B., & Laget, M. 1995, A&A, 303, 661
Fabian, A.C., Nulsen, P.E.J., & Canizares, C.R. 1984, Nat, 310, 733
Fabian, A.C., 1994, ARA&A, 32, 277
Gunn, J.E., & Gott, J.R.I., 1972, ApJ, 176, 1
Hansen, L., Jorgensen, H.E., & Norgaard-Nielsen, H.U. 1998, Ap&SS, 257, 311
Heckman, T.M., Baum, S.A., van Breugel, W.J.M., & McCarthy, P. 1989, ApJ, 338, 48
Kennicutt, R.C. 1998, ARA&A, 36, 189
Koekemoer, A.M., O'Dea, C.P., Sarazin, C.L., McNamara, B.R., Donahue, M., Voit, M., Baum, S.A., & Gallimore, J.F. 2002, NewAR, 46, 149
Koratkar, A., Evans, I, Pesto, S., & Taylor, C. 1997, /apj, 491, 536
Leitherer, C. et al. 1999, ApJS, 123, 3
Mason, K.O. et al. 2001, A&A, 365, L36
McNamara, B.R. & O'Connell, R.W. 1989, AJ, 98, 201
McNamara, B.R. et al. 2000, ApJ, 534, 135
McNamara, B.R., Wise, M.W., & Murray, S.S. 2004, ApJ, 601, 173
McNamara, B.R. 2004, astro-ph/0402081
Melnick, J., Gopal-Krishna, & Terlevich, R.J. 1997, A&A, 318, 337
Miller, N.A. & Owen, F.N. 2003, AJ, 125, 2427
Moore, B., Katz, N., Lake, G., Dressler, A., & Oemler, A., Jr., 1996, Nat, 379, 613
Mittaz, J.P.D. et al. 2001, A&A, 365, L93
O'Dea, C.P., Baum, S.A., Mack, J., & Koekemoer, A.M. 2004, ApJ, 612, 131
Peterson, J.R., Kahn, S.M., Paerels, F.B.S., Kaastra, J.S., Tamura, T, Bleeker, J.A.M., Ferrigno, C., & Jernigan, J.G. 2003, ApJ, 590, 207
Rosa-Gonzalez, D., Terlevich, E., & Terlevich, R., 2002, MNRAS, 332, 283
Sarazin, C.L., 1986, Rev. Mod. Phys., 58, 1
Sarazin, C.L., Burns, J.O., Roettiger, K., & McNamara, B.R. 1995, ApJ, 447, 559
Smith, E.P., Bohlin, R.C., Bothun, G.D., O'Connell, R.W., Roberts, M.S., Neff, S.G., Smith, A.M., & Stecher, T.P. 1997, ApJ, 478, 516
Vassiliadis, E. et al. 1996, ApJS, 105, 375
Voigt, L.M. & Fabian, A.C. 2004, MNRAS, 347, 1130

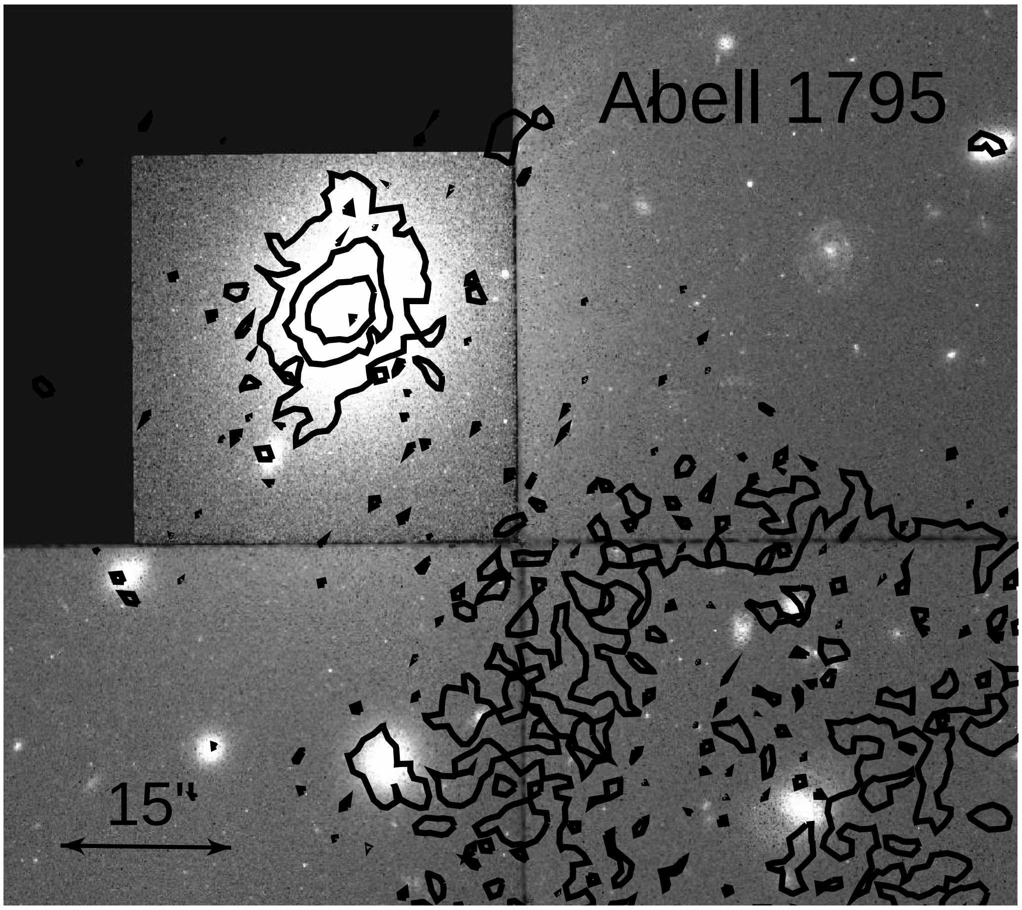

Fig. 1.— HST WFPC2 1780 sec exposure of Abell 1795. This image has been overlaid with UV contours from an XMM-Newton Optical Monitor observation. Logarithmic contours in black were produced with a 2499 second exposure image, and have count values of 14, 25, 44.75, and 80. The large splotch of UV contours to the lower right of the cD galaxy is due to scattered light.

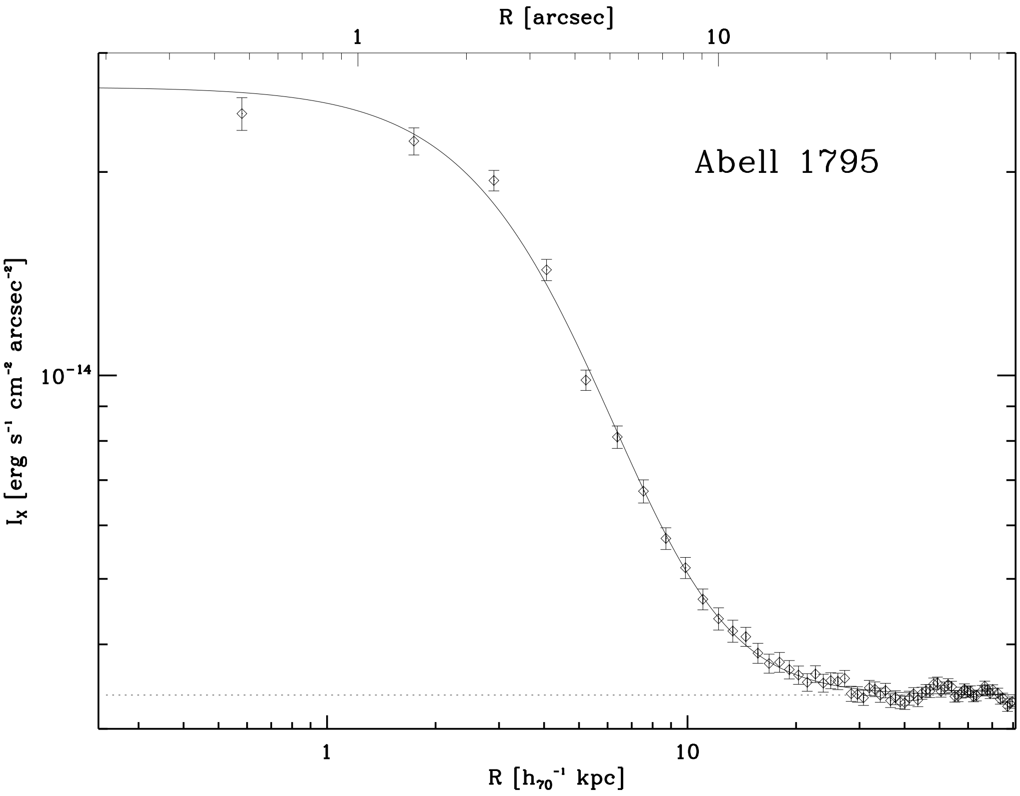

Fig. 2.— **Surface Brightness Profile.** Radial surface brightness profile of Abell 1795 made from UVW1 (220-400 nm) data accumulated in $\sim 1''$ annular bins. A solid line traces the best β model fit. The horizontal dotted line represents the best fitting background value. The best fitting β model has a core radius of 4.09 $''$ and beta value of 0.703

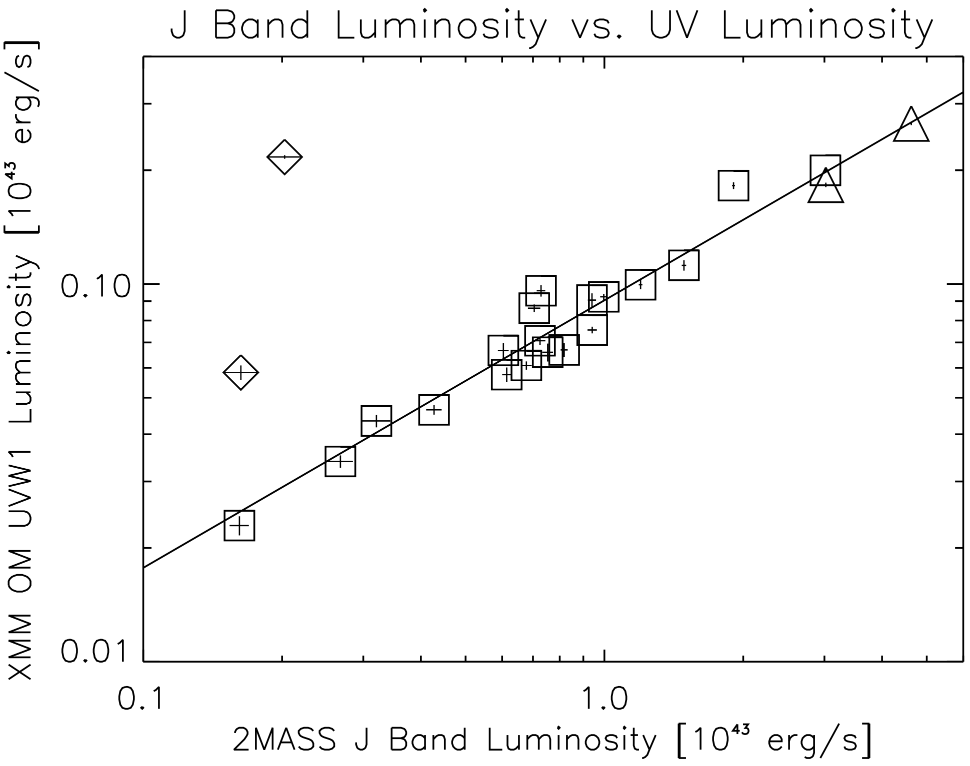

Fig. 3.— UV vs. IR luminosity for non-cooling flow cluster galaxies in our sample. The line indicates the best fitting relationship between UV and IR luminosity for passively evolving and non-cooling flow cD galaxies, represented by squares and triangles, respectively. Diamonds indicate two star forming galaxies which were excluded from the fit. A relationship between UV and IR luminosity is expected here, because passively evolving cluster galaxies have similar spectral energy distributions (SEDs). The similar redshifts of IC1860 and Coma allow us to fit this relationship without making distance corrections to the data.

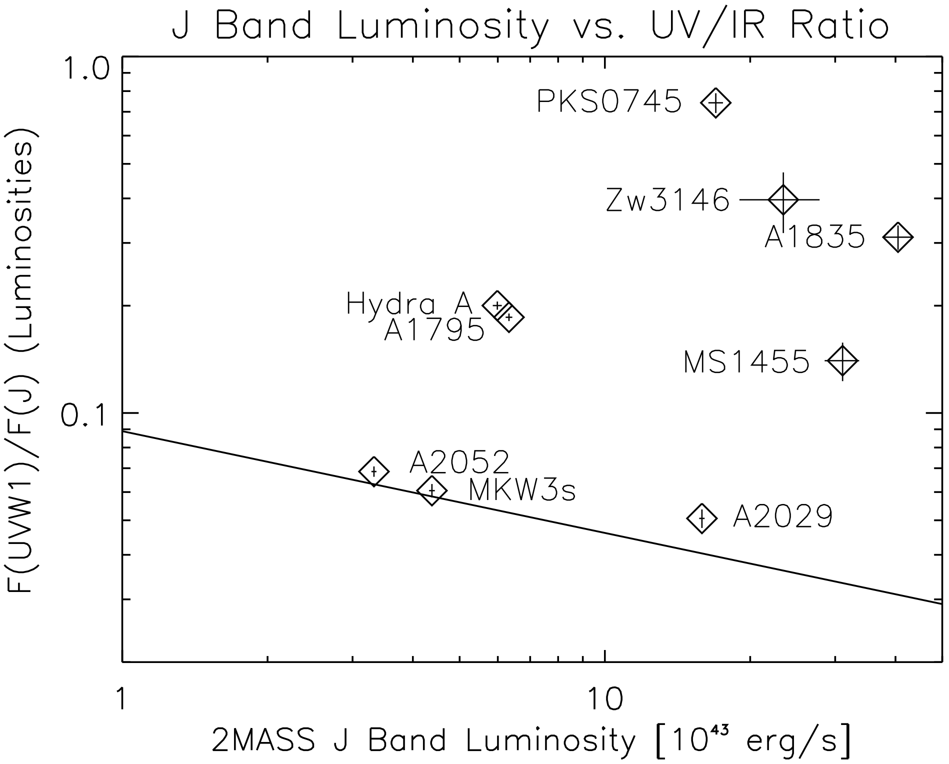

Fig. 4.— UV/IR luminosity ratio vs. 2MASS J band luminosity. All luminosities were calculated in 7″ radius regions, and corrected for galactic extinction. Diamonds indicate cooling flow cluster cDs, all of which are at low redshift ($z < 0.1$) except for the three points farthest to the right, which have redshifts of ~ 0.25. The line designates the best fitting relationship between UV and IR luminosity for passively evolving and non-cooling flow cD galaxies (Section **??**). The high UV/IR ratio of the cooling flow clusters is a strong indication of the existence of hot young stars and thus a direct indication of copious recent star formation.

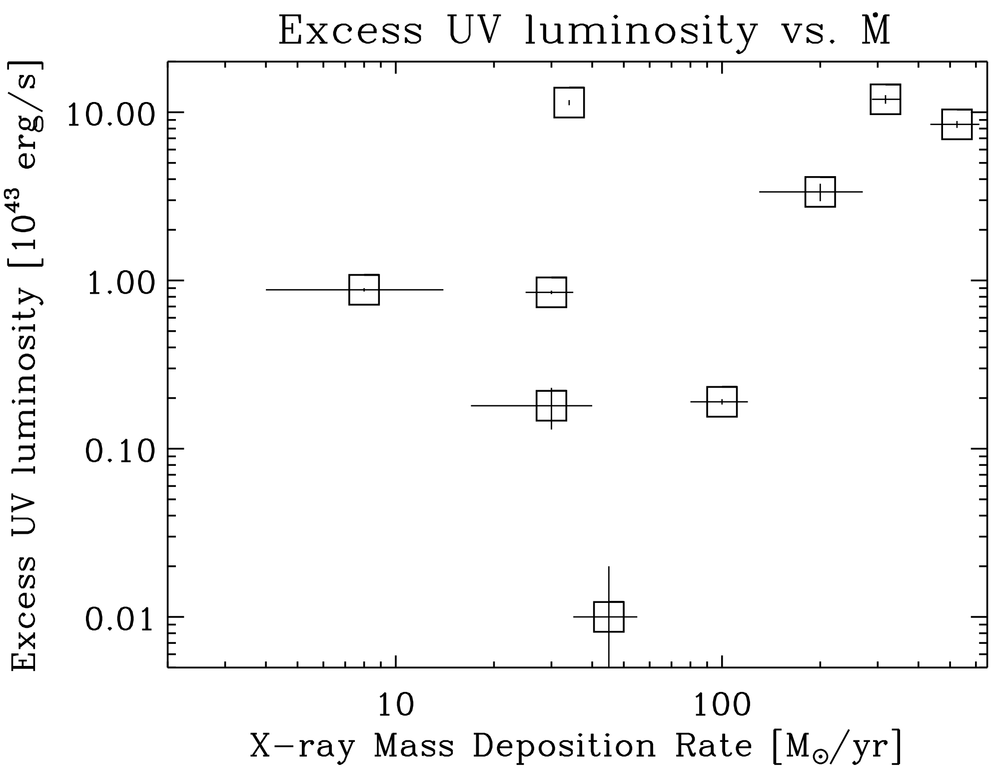

FIG. 5.— Excess UV luminosity vs. $\dot{M}$. Luminosity excesses were determined by subtracting the best fit ratio of UV light due to old stars (Figure 2) from the measured UV luminosity of each cluster. X-ray mass deposition rates were taken from recent papers (Peterson et al. 2003; Voigt & Fabian 2004).

TABLE 1
XMM-Newton Optical Monitor Observations

Object	z	Filter(s)	Exposure [s]
IC 1860	0.0229	UVW1	5000
PKS 0745-191	0.1028	UVW1	3999
Hydra A	0.0538	UVW1	3000
Zw3146	0.2906	UVW1	4000
NGC 4406 (M86)	-0.0008	UVW1 (UVM2)	3600 (3500)
NGC 4472 (M49)	0.0033	UVW1 (UVM2)	2000 (1000)
NGC 4649 (M60)	0.0037	UVW1 (UVW2)	2499 (2900)
Coma (center)	0.0231	UVW1	3900
Coma (outskirts)		UVW1	1498
Abell 1795	0.0633	UVW1	2499
Abell 1835	0.2520	UVW1	2000
MS 1455.0+2232	0.2578	UVW1	2000
Abell 2029	0.0779	UVW1	1200
Abell 2052	0.0345	UVW1	2000
MKW3s	0.0453	UVW1	2002

TABLE 2
BETA-MODEL FITS

Object	$R_{\rm core}$ [$''$]	β	I_0[a]	$I_{\rm B}$[a]	Reduced χ^2
PKS 0745-191	$2.83^{\pm 0.04}$	$0.766^{\pm 0.011}$	$625.3^{\pm 12.4}$	$481.0^{\pm 1.6}$	0.691
Hydra A	$3.449^{\pm 0.001}$	$0.8387^{\pm 0.0002}$	$4829.1^{\pm 2.4}$	$356.59^{\pm 0.06}$	4.200
Zw3146	$6.21^{\pm 0.01}$	$2.054^{\pm 0.007}$	$1119.2^{\pm 4.3}$	$413.2^{\pm 0.4}$	0.947
Abell 1795	$4.09^{\pm 0.01}$	$0.703^{\pm 0.002}$	$2334.8^{\pm 13.4}$	$336.6^{\pm 0.3}$	0.946
Abell 1835	$3.65^{\pm 0.41}$	$1.253^{\pm 0.165}$	$2880.7^{\pm 153.0}$	$349.6^{\pm 1.8}$	0.514
MS1455.0+2232	$4.99^{\pm 0.03}$	$1.006^{\pm 0.007}$	$446.9^{\pm 3.5}$	$337.8^{\pm 0.4}$	0.657
Abell 2029	$3.68^{\pm 0.02}$	$0.499^{\pm 0.001}$	$613.2^{\pm 3.5}$	$449.7^{\pm 0.6}$	1.101
Abell 2052	$1.68^{\pm 0.28}$	$0.402^{\pm 0.022}$	$1593.1^{\pm 149.6}$	$426.2^{\pm 7.4}$	1.912
MKW3s	$1.28^{\pm 0.33}$	$0.352^{\pm 0.022}$	$1018.0^{\pm 138.9}$	$398.6^{\pm 7.1}$	1.110

[a]Surface brightness I in units of 10^{-17} ergs sec^{-1} cm^{-2} arcsec^{-2}

TABLE 3

Cluster	z	UV Excess $[10^{43}$ erg/s]	$\dot{M}_{2.35}$ [a] $[M_{\odot}/\mathrm{yr}]$	$\dot{M}_{3.3}$ [a] $[M_{\odot}/\mathrm{yr}]$	$\dot{M}$ (X-ray) $[M_{\odot}/\mathrm{yr}]$	τ_{sf} [Myr]	α
PKS 0745-191	0.1028	$11.94^{\pm 0.7}$	$129^{\pm 7}$	$237^{\pm 13}$	317^{+35}_{-29} [b]	200	3.3
Hydra A	0.05384	$0.88^{\pm 0.02}$	$9.5^{\pm 0.2}$	$17.5^{\pm 0.4}$	8^{+6}_{-4} [b]	900^{+}	2.35
Zw3146	0.2906	$8.47^{\pm 0.4}$	$91^{\pm 4}$	$168^{\pm 8}$	525^{+90}_{-90}	11	3.3
Abell 1795	0.06326	$0.85^{\pm 0.02}$	$9.1^{\pm 0.2}$	$16.7^{\pm 0.4}$	30^{+5}_{-5} [b]	100	3.3
Abell 1835	0.251982	$11.41^{\pm 0.4}$	$123^{\pm 5}$	$226^{\pm 9}$	34^{+43}_{-34} [b]	900^{+}	2.35
MS 1455.0+2232	0.2578	$3.36^{\pm 0.4}$	$36^{\pm 4}$	$66^{\pm 8}$	200^{+70}_{-70}	150	3.3
Abell 2029	0.07795	$0.18^{\pm 0.05}$	$1.7^{\pm 0.5}$	$3.2^{\pm 0.9}$	30^{+10}_{-13} [b]	7	3.3
Abell 2052	0.03446	$0.19^{\pm 0.007}$	$0.19^{\pm 0.08}$	$0.4^{\pm 0.1}$	100^{+20}_{-20} [c]	...	...
MKW3s	0.04531	$0.01^{\pm 0.01}$	$0.1^{\pm 0.1}$	$0.2^{\pm 0.2}$	45^{+10}_{-10} [c]	...	...

[a]Assuming constant star formation over 900 Myr. The subscript indicates the IMF powerlaw slope of the model used. [b]Voigt & Fabian (2004). [c]Peterson et al. (2003).